Air/ liquid interface assisted self-assembly of polyindole via Langmuir-Blodgett system

3.1 Introduction

The advent in necessity of polymer based thin films devices in modern flexible electronics prominently rely on the high performance and ubiquitous functionality of p-conjugated semiconducting polymers. However, the major hurdle in their practical execution is their poor performance in comparison to conventional silicon based devices. Updating with the trend of performance refinement of conductive polymer based devices, the importance of tailoring technique or molecular engineering apart from employing suitable synthetic route cannot be undervalued at any cost. Post-synthesis molecular engineering technique regulates charge mobility governing factors such as functionality, structural order, orientation and alignment of polymer chains to a large extent, so it urges for its smarter selection [53,54,56,57,64,95,96]. As is well known fact, that polymeric materials are already merited with economical synthesis steps. Here, we are highlighting the significance of post-synthesis fabrication techniques that can precisely control the chain ordering of polymeric materials and simultaneously monitor their film morphology to obtain an orientated large area thin films.

Supremacy of LB technique over other fabrication techniques such as drop casting, spin coating, etc. has been undoubtedly accepted worldwide. Desire for self-assembly of organic molecules with a greater level of structural control to obtain ordered film over a large area has been very well satisfied exploiting this technique in last few decades [53,54]. In addition to positioning certain molecules at precise distances with respect to neighbouring molecules, this technique endows an opportunity to exercise molecular-level control over the orientation of molecules in monolayer that affects the

structure and thickness of the films [42,55,67,97,98,99]. This pressure-controlled thin film fabrication LB technique unlocks a wide range of application for CP thin films such as capacitors, biosensors, field effect transistors, gas sensors, chemical sensor, etc. [42,53,54,58]. To the best of our knowledge, we are the first to explore the self-organizing properties of unsubstituted PIn with smart LB technique to obtain its ordered films for various characterizations and charge transport study.

It is well known fact, that greater the amphiphilicity of material for LB film, easier is its molecular orientation and greater is the film stability. This utmost requirement for LB is fulfilled by the presence of heteroatom N in the indole monomeric unit providing it polarity thus rendering it hydrophilic. LB film quality of conductive polymers that donot possess alkyl substituent fall short of stability and uniformity (transfer ratio <1). This issue can be addressed by two ways, first by mixing with a small quantity (~5-10%) of long chain fatty acid (surfactant) to obtain stable mixed monolayer film and second via precursor route i.e. derivatization of monomer with alkyl chain prior to polymerization [53,54,58]. Both the above methods enhance the solubility of the polymer prior to LB film preparation and the film stability as well. Meanwhile, resolving stability and solution processability issues, these films are cursed with a demerit i. e. these chains start acting as good insulators that can pose serious obstruction in charge transport perpendicular to the film and dilute the effect of functional groups in the film. In some reports, the alkyl chains embedded into material via synthetic route have been removed thermally after deposition of LB films [53,54,58]. But post heat treatment may harm functional integrity of the molecule in case of conductive polymers. Keeping this in view, we have avoided incorporation of any surfactant or post heat treatment to obtain the LB films of unmodified/ unsubstituted PIn without compromising with its conductivity and

to protect the functional integrity of the material with consideration of various factors necessary for its film stability.

Recently, PIn (inset of Figure 3.1(a)) and its derivatives being a new class of conductive polymers, have attracted significant scientific interest due to its ease in synthesis via chemical and electrochemical route, excellent redox activity, thermal stability, low toxicity, good electrochromic properties, electrocatalytic properties, electronic property and sensing property [51,69]. However, their two most important downsides i. e. poor conductivity and poor solubility in common volatile organic solvents have plagued them for practical applications and fabrication of devices. Though, various nanocomposites of PIn have been prepared which exhibit good electro catalytic activity, photoelectrochemical property as well as better electrical properties [69,79-82]. Still, the issue of solution processability and poor conductivity hang on the major limiting factor for its broad practical applications.

In the present work, we tried to resolve the processability issue of unsubstituted PIn to much extent by employing the concept of co-solvent methodology i. e. dissolving in one solvent DMSO which acts as good solvent followed by transfer in other common volatile organic solvent (chloroform). After that, we opted LB technique to obtain its stable and well-ordered film (without utilizing any external template) with very smooth surface and further investigated its layer dependent charge transport property and better electronic device parameter.

3.2 Results and Discussion

3.2.1 Molecular Studies

Electrochemically synthesized PIn was characterized via ^{1}H-NMR and FT-IR

spectroscopy for its 2,3-linkage and NH bond existence. Figure 3.1 (a) indicates proton chemical shift (δ-value) at 10.93 ppm validating the existence of NH bond [51,76]. Other peaks at δ-values around 8.08, 7.86, 6.95 and 6.78-6.38 ppm correspond to H-4, H-7, H-5 and H-6 aromatic protons of monomeric unit that are persistent in PIn respectively. These values are in accordance to previous reports, thus verifying the 2,3-linkage in PIn [51,69,76]. Vibrational spectrum for electrpolymerized PIn (as shown in Figure 3.1 (b)) displays a broad peak at ~3400 cm^{-1} depicting NH bond stretch. Also, NH bond deformation at 1610 cm^{-1} validate its persistence after polymerization. Peaks around 1600-1400 cm^{-1} region peaks arise due to C-C stretching modes of benzene ring.[19] Peak at 1103 cm^{-1} designates to aromatic C-N stretch and peak at 736 cm^{-1} (C-H bend; out-ofplane deformation) validates non-involvement of benzene ring in polymerization [51,69,76]. In conclusion, N-H peak presence verifies that nitrogen is not the polymerization site. ^{1}H-NMR along with FT-IR spectra is verifying the 2, 3-linkage of indole moiety during electrochemical polymerization. Mass spectrum of PIn (as shown in Figure 3.2) was examined via FAB mass technique that revealed the heaviest ion to have m/z value of 1036. Since the largest m/z value represents the largest ion going through the mass spectrometer and hence it was the molecular ion. Therefore the mass of PIn was considered to be 1036 which indicates the association of 8-9 monomer units in the polymer chain.

3.3.2 Isotherm studies

The formation of polymer films at the air-water interface is very sensitive and largely depends on preparation conditions such as solvent, concentration, temperature of subphase, compression speed, etc. [53,54,58]. Figure 3.3 depicts the typical LB π-A isotherm for PIn molecules at room temperature depicting decrease in mean monomeric

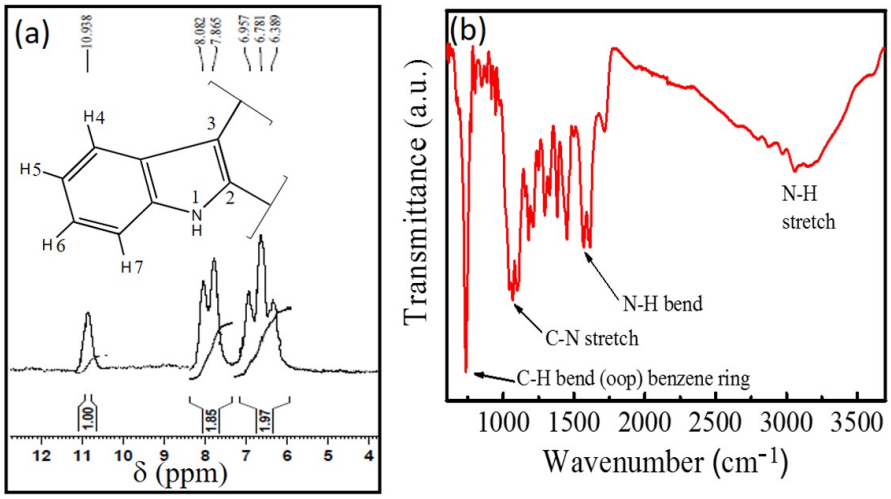

Figure 3.1 (a) ^{1}H-NMR spectrum and (b) FT-IR spectrum of electrochemically synthesized PIn.

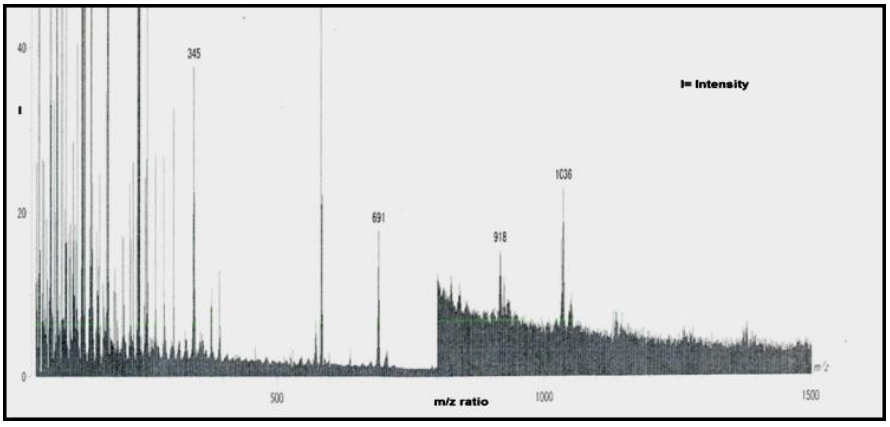

Figure 3.2 FAB Mass spectrum of electrochemically synthesized PIn.

area with increase in pressure. A very dilute solution (dispersion; 200 mL of 1.0 mg/mL) of PIn (shown in inset Figure 3.3) was spread using Hamilton microliter syringe over water subphase and was left over for 15 min for complete polymeric chain extension along with solvent evaporation. Then after, the barriers were compressed at 10 mm/min speed and the SP was monitored via Wilhemy plate method to explore the isotherm. Isotherm investigation was repeated 3-5 times keeping various parameters such as temperature, concentration, pH of subphase and compression speed constant. Each time

we obtained the similar results with negligible differences ensuring the stability of monolayer at the water subphase.

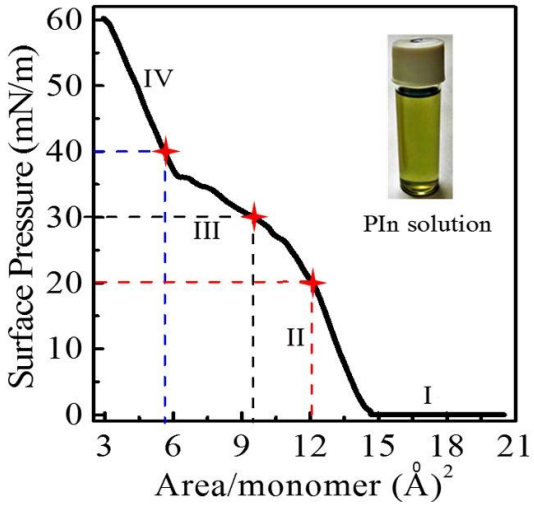

Figure 3.3 Pressure vs. area (π-A) isotherm of PIn at room temperature (marked points display different pressures 20, 30 and 40 mN/m under study). Inset shows photograph of PIn solution prepared for LB study.

The π-A isotherm started lifting off at 14.70 $(Å)^2$/ repeat unit around 0.12 mN/m and SP continued to increase upto 60.02 mN/m after which it started decreasing which can be allocated as the collapse point. There are 3 slope changes occurring at the area per monomer of 14.52, 12.08 and 6.22 $(Å)^2$ observed in Figure 3.3 denoting phase transition phenomena. On this basis, the entire isotherm can be allocated into four distinct sections as mentioned in some previous reports [18,53-55,63,76]. The region I (upto 0.12 mN/m) is allocated as gaseous state, where there is almost no alteration in the SP. Further, from 0.12 mN/m to 20 mN/m is assigned as liquid phase marked as region II. Further rise in pressure from 20 mN/m to 35mN/m is marked as region III (plateau region) and allocated as a collapsed liquid condensed phase. A steep rise in the SP is observed on further compression of barrier and assigned as region IV (solid phase) that extends upto 60 mN/m

(collapse pressure). Here, it is worth mentioning that the area/monomer is very less in comparison to actual area of monomer. According to previous studies, aromatic molecules without any hydrocarbon tail do not form true monolayers [53,54]. Therefore, it is quite obvious that the PIn monolayer forming over water surface is pseudo-monolayer consisting of several molecule thicknesses. These pseudomonolayers form Z-type deposition films with upstroke lifting on hydrophilic substrate [53,54]. Based on number of layers transferred on ITO substrate, they have been named as single layer, 3 and 5 layers to investigate their charge transport property discussed later. Area per monomer values at 20, 30 and 40 mN/ m are 12.02, 9.50 and 5.60 mN/m (intersection of dotted line on x-axis in Figure 3.3). Amongst the lowest SP selected for film investigation i. e. 20 mN/m, the largest area per monomer observed corresponds to lowest surface density. As the SP is increased, surface density increases upto some extent after which the film starts overlapping/ folding beyond 40 mN/m. This was clearly evidenced via Figure 3.4 AFM and SEM micrographs discussed later.

3.3.3 Surface morphology studies at different pressures

The surface roughness, height profile, surface morphology, etc. of transferred films were characterized and estimated using AFM and SEM. Figure 3.4 (a, c and e) shows the AFM topography (tapping mode) and Figure 3.4 (b, d and f) shows the SEM image of PIn LB film transferred at 20, 30 and 40 mN/m SP, respectively. LB film AFM image at 20 mN/m in Figure 3 (a) displays long grooves which is clearly shown by breaks in corresponding SEM image (Figure 3.4 (b)). The inset of later displays the magnified image revealing that PIn molecules form islands on water subphase with gaps in between, thus film deposited at this pressure is not compact enough. Figure 3.4 (c) AFM image of LB film lifted at 30 mN/m indicates very clearly, the formation of very smooth, continuous and

condense film which is supported by its SEM image (Figure 3.4 (d)) [55,76]. In order to check the film compactness at higher pressures, the film was also lifted at 40 mN/m. Their AFM (Figure 3.4 (e)) and SEM (Figure 3.4 (f)) images clearly exhibit the folding or collapse of the film on application of higher pressure which is also observed as steep rise in isotherm obtained for PIn discussed earlier [55,76]. Thus, AFM and SEM images

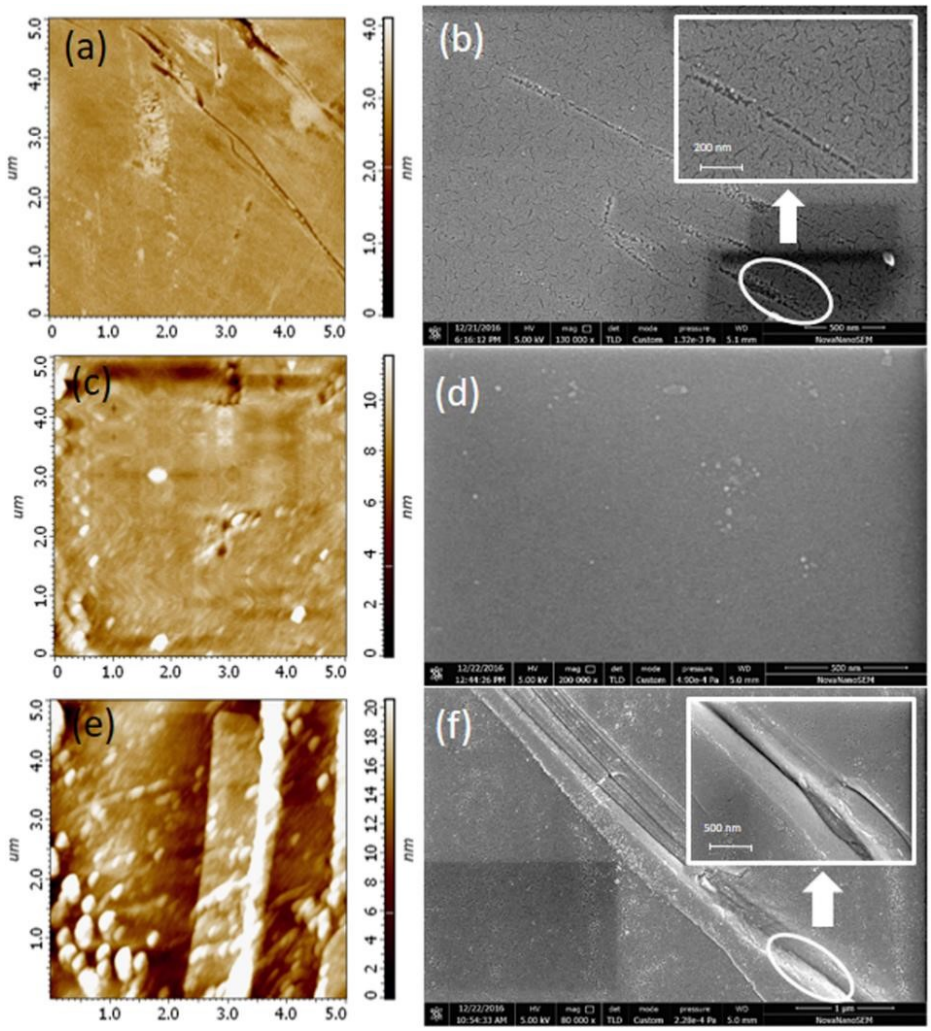

Figure 3.4 Tapping mode AFM and SEM images of monolayer LB film of PIn at different deposition pressures (as marked in isotherm) (a & b) @ 20 mN/m, (c & d) @ 30 mN/m, (e & f) @ 40 mN/m respectively. Each inset shows the magnified image encircled region.

together very well justify 30 mN/m pressure (as obtained in isotherm, Figure 3.3) as the optimum one to obtain most compact PIn LB films for the charge transport study.

Investigation of uniformity and smoothness of large area single layer LB film (at 30 mN/m) was also done via SEM and AFM image (as shown in Figure 3.5 (a) and (b)). In addition, Figure 3.6 displays topographic AFM 3D images of the same AFM substrates as observed in Figure 3.4 (a, c and e). Figure 3.6 (a) reveals the gap formed at lower SP (20 mN/m) and Figure 3.6 (b & c) display some spikes that are more for the later case.

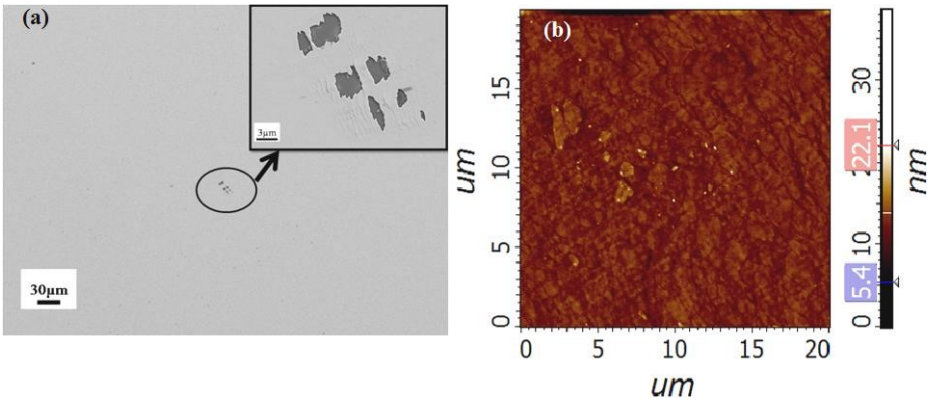

Figure 3.5 (a) SEM image of single layer LB film of PIn. Inset shows the magnified image encircled region (b) AFM image of single layer LB film of PIn.

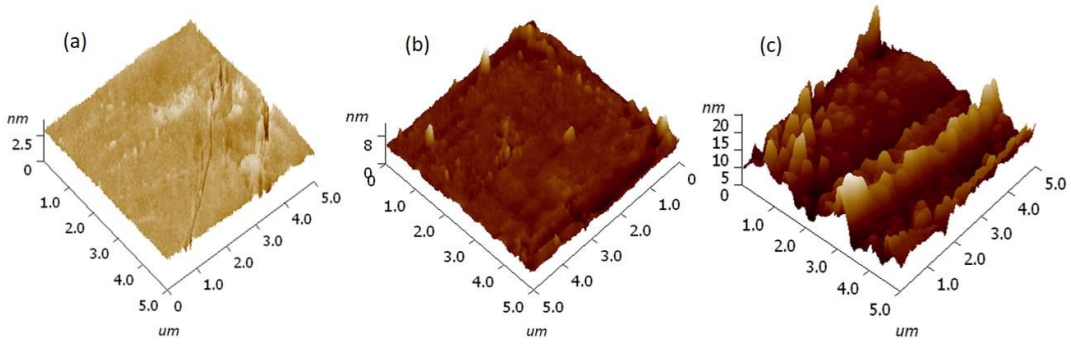

Figure 3.6 Topographic AFM 3D images of monolayer PIn LB film deposited at different SP (a) 20 mN/m, (b) 30 mN/m, (c) 40 mN/m respectively.

Table 3.1 compares RMS roughness values for Figure 3.6 (a-c) images. Highest RMS roughness values for 40 mN/m deposited film clearly justify the presence of more spikes [55,76]. This led to the conclusion that most homogenous morphological pattern is obtained for 30 mN/m (Figure 3.6 (b)). Thus, smooth and compact large area (~600 x 600 mm^2) PIn LB film micrographs very much motivate for their implementation in large area application devices.

Table 3.1 Roughness (RMS) and average height measurement of PIn LB monolayer film.

LB film sample	RMS roughness (nm)
(a) 20 mN/m	0.236
(b) 30 mN/m	0.643
(c) 40 mN/m	2.468

Based on above results, we designed a schematic representation (as shown in Figure 3.7) of LB trough equipped with double barriers where PIn solution is spread dropwise onto water subphase. It represents the plausible arrangement of PIn molecules on subphase at different SP (20, 30 and 40 mN/m). PIn molecules being apart at 20 mN/m start coming closer on further barrier compression. At 30 mN/m, they are equidistant to each other forming compact arrangement. On further increasing pressure (at 40 mN/m) molecules overlap each other, thus disrupting the film continuity.

3.3.4 Spectral studies

Figure 3.8 (a) shows the typical UV-Vis absorption spectrum of PIn in solution (dispersion) and PIn LB film coated on optically transparent quartz substrate at 30 mN/m. Since, the monomer unit of PIn consists of rings having π-conjugation/electrons with nitrogen as hetero atom consisting of non-bonding orbital. This type of molecule shows n-π* excitation as a lowest energy transition level. However, oxidative polymerization of

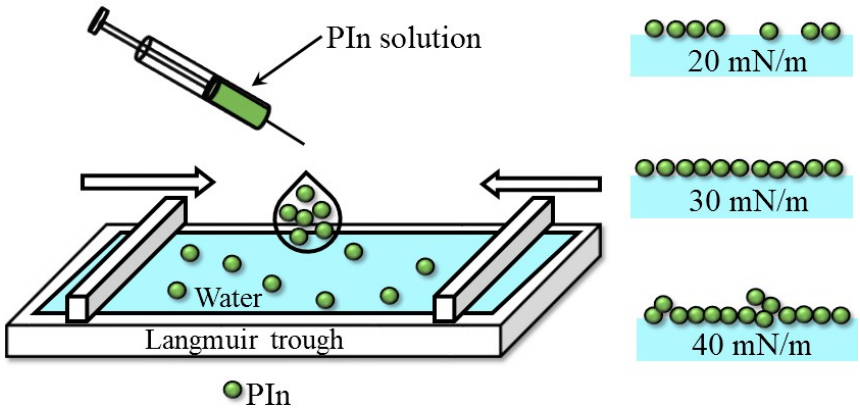

Figure 3.7 Schematic representation of plausible arrangement of PIn molecules onto water subphase at different SP (20, 30 and 40 mN/m).

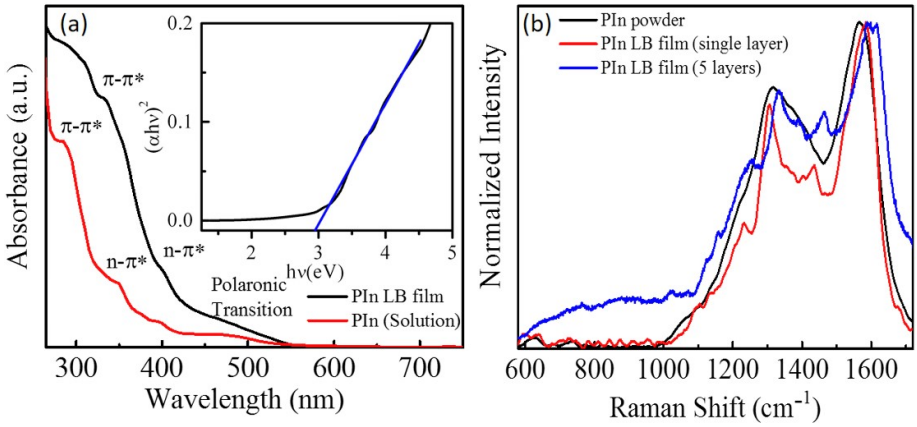

Figure 3.8 (a) UV-Vis absorption spectra of PIn (solution) and LB film of PIn with inset depicting its band gap.(b) Raman spectra of PIn (Powder) synthesized electrochemically and PIn LB film (monolayer and 5 layers), respectively.

these molecules causes generation of defects over polymer chains in the form of polarons. The polaron shows lower energy transition in comparison to π-π* and n-π *. Therefore, the peaks observed for PIn in solution and its LB film both can be assigned as π-π* (270-340 nm), n-π* (340-400 nm) and 465-475 nm as a polaronic excitation [51,55,63,76]. As compared to liquid phase spectra, there is bathochromic shift for LB film clearly indicating the enhanced self-assembly and structural ordering in the film. LB technique

allows ample time and space for PIn molecules to orient themselves such that when barriers are gradually compressed, non-covalent forces come into action facilitating their ordered array. Thenafter, band gap (E_g) of PIn LB film was calculated from the absorbance spectra of the PIn (inset of Figure 3.8 (a)). If absorption coefficient is denoted by a, energy of absorbed light is denoted by hv then optical bandgap of the polymer is estimated by fundamental relation given by [51,100]

$$\alpha h\mathcal{V} = B(h\mathcal{V} - E_g)^n \qquad (3.1)$$

Where α and $h\mathcal{V}$ denote absorption coefficient and energyof incident absorbed light, n=1/2 for direct band gap transition, and B denotes the proportionality constant. Energy gap, E_g is predicted by plotting $(\alpha h\mathcal{V})^2$ vs. $h\mathcal{V}$ and extrapolating the linear portion to zero, as shown in inset of Figure 3.8 (a). The band gap of PIn LB film is predicted to be 2.9 eV using this manner.

Raman spectroscopy was used to investigate the selfassembly and possible improvement in ordering of the PIn films deposited by the LB technique and contemporarily compared with the electropolymerized PIn as shown in Figure 3.8 (b). It is important to note that, bare ITO did not show any well resolved peaks (very low intensity peaks) which is consistent with our previous report [51]. However, only two broad peaks at 1315 and 1567 cm^{-1} were observed for electropolymerized PIn over the same ITO coated glass. [55,82]. PIn LB film (single and 5 layers) displays two major peaks with slight shift (~15-20 cm^{-1}) towards higher wavenumber in comparison to electropolymerized PIn with some additional small peaks on shoulders of the major peaks.

The acquired outcomes for LB PIn films and electropolymerized PIn can be defended on the basis of enlightenments that electropolymerization is a relatively faster technique (less than 100s at ~1.2 V). Thus, polymer chains do not get enough time to assemble in an ordered fashion that stem into amorphous state exhibiting only two broad peaks.

Whereas, a number of shoulder peaks observed in the case of the LB film (both single and 5 layers) appeared due to strong interactions between the ordered chains [55]. Red shift was observed more for 5 layers as during first layer deposition, the substrate nature decides the adhesion pattern of material onto it. But in the case of multilayers, the polymer film itself acts as substrate that has better cohesion property, thus improving the ordering [67]. Piwowar et al. and Murphy et al. have already estimated the change in configuration and structure via spectroscopic measurements [98,101]. The presence of shoulder peaks can be enlightened via investigating the interaction at molecular level that was explored via isotherm study prior to film deposition via LB technique. It is very important to employ a very dilute PIn solution (~ 0.5-1 mg/mL) for spreading at air-water interface in order to provide sufficient room for polymeric chain extension. The compression speed (10 mm/min) of the barriers was also kept extremely low to complement the self-organizing property of PIn chains at molecular level. Both presence of -NH group in monomeric unit of PIn and possibility of π-π interaction play a vital role in directing the orientation and ordering of PIn over the subphase [55,62]. The -NH group being polar aids in definite orientation of PIn chain over the water surface and is the driving force for solvent spreading. The two forces i.e. cohesive (van der Waals interaction) attraction amongst PIn molecules and the attractive interaction between polar end of PIn and subphase determines the monolayer characteristic. In this circumstance, the polymer chains may come closer retaining a definite alignment due to slow compression thus getting enough time to form an ordered array (as shown in Figure 3.7). It is also worth mentioning here that one group i. e. Chang et al has reported about the dependency of self-assembly of polymer chain on boiling point and drying time of solvent [102]. In their report, they have clearly mentioned the effect of time on crystallinity and ordering of polymer film.

3.3.5 Charge Transport and electronics parameter analysis

The charge transport and electronic parameter of layer by layer deposited LB films of PIn were studied across the film using sandwiched structure of Al/PIn/ITO (inset of Figure 3.9 (a)) via conducting the J-V measurement in dark condition. Measurements were performed at room temperature (27 °C) in air under dark conditions as shown in Figure 3.9 (a-b), in which Figure 3.9 (b) shows the semilog plot of log J vs. V depicting high rectification behaviour of diode. The rectifying behaviour of the sandwiched structure devices Al/PIn/ITO were analysed by assuming the standard thermionic emission theory and diode parameter were extracted based on these equations [100,103].

$$\mathrm{J} = J_0 \left[\exp\left(\frac{\mathrm{qV}}{\eta \mathrm{kT}}\right) - 1\right] \qquad (3.2)$$

Where η and J_0 denote ideality factor and saturation current density. At room temperature, the value of J_0 can be ignored, so the equation becomes,

$$\mathrm{J} = J_0 \left[\exp\left(\frac{\mathrm{qV}}{\eta \mathrm{kT}}\right)\right] \qquad (3.3)$$

$$\eta = \frac{q}{kT}\left(\frac{\partial V}{\partial \ln(J)}\right) \qquad (3.4)$$

$$J_0 = \mathrm{A} * \mathrm{T}^2 \exp\left(\frac{-q\emptyset_B}{KT}\right) \qquad (3.5)$$

Where A* denotes effective Richardson constant which is equal to 120 A/cm^2 for free electron. Rectification ratio is defined as forward current/reverse current. The calculated electronic parameters such as saturation current density J_0, barrier height φ_B, ideality factor η and rectification ratio listed in Table 3.2.

It is important to note that maximum forward current density was observed in single layer LB film however, layer by layer deposition of LB film cause reduction in current (Figure 3.9 (a)) with incremenet in turn on voltage (Table 3.2) with inceasing the number of

Table 3.2 Electronic parameters of devices.

Parameter→ Devices ↓	**Turn on voltage (V)**	**H**	**J_0 (A/cm^2)**	**Φ_B (eV)**	**Rectification ratio**
1 layer	1.40	2.0	6.52x 10^{-9}	0.95	46
3 layers	1.80	3.3	2.64x10^{-10}	1.03	91
5 layers	2.15	4.8	1.07x10^{-10}	1.05	793

layers. It is also observed that there is sharp decrement in maximum forward current as compare to number of layers as shown in Figure 3.9 (a). Ordered polymer chains were obtained in single layer PIn LB film which cause significant enhancement in current due to well electronically coupled chain. Further, it is noteworthy that layer by layer deposition of PIn LB film occur via only physical adsorption i.e there is no electronic coupling between layers and polymer of two layers. It is also noteworty that layer by layer depostion cause reorientation of molecule because of change of nature of substrate after first layer depostion. Raman spectra as shown in Figure 3.8 (b) also confirms the change in orientation of molecule. Therefore, there exist a energy barrier between the layers which increase the resistanece across the film. Thus, this sharp decrement in current across the film arises due to formation of energy barrier at interface of two successive deposited self-assembled film during deposition and change in orientation of film in layer by layer depositions as confirmed by Raman spectra (Figure 3.8 (b)). Similar observation were also seen in our previous report [55,67].

Further, the ideality factor of devices Al/PIn/ITO fabricated by using LB films are higher in comparison to ideal diode ideality factor (=1). In general, carrier drift diffusion process and the Sah–Noyce–Shockley generation recombination process produce ideality factors between 1.0 and 2.0 [104]. The exceeding value of ideality factor from 2.0 originates

from several phenomena such as trap-assisted tunnelling, carrier leakage, and barrier inhomogeneity etc. Layer by layer deposition of PIn LB film cause incorporation of some other recombination centre as mentioned such as trap-assisted tunnelling, carrier leakage, and barrier inhomogeneity etc excluding carrier drifft diffusion and Sah-Noyce-Shocley. Therfore, multilayer LB films devices show ideality factor more than 2 probably due to increase in trap-assisted tunnelling, carrier leakage, and barrier inhomogeneity resulted on multilayer formation during layer by layer deposition as shown in Figure 3.9 (b) [105]. Therefore, multilayer deposited PIn LB films devices show the deviation from ideal behaviour which is consistent with our previous assumptions [67].

The current obtained for Al/PIn/ITO configurations (single layer) is higher than multi-layered PIn LB devices. LB film devices show high current density. Ordered polymer chains cause significant enhancement in current. Forment et al. has reported that barrier height will reduce with the smoothness of surface. Since, layer by layer deposition of PIn LB films cause reduction in smoothness that results in increase in barrier height and reverse saturation current [106].

Finally, it is important to note that the rectification ratio of PIn LB film rises with increase in number of layers. The increment in rectification ratio can be justified due to formation of island over subphase and due to this phenomenon, leakage current is high in reverse bias condition. Increasing the number of layers causes reduction in leakage current, resulting in higher rectification ratio with decrease in forward current.

Thus, LB technique for formation of PIn thin films over substrates for construction of devices exhibits great potential for broad area electronic applications and may be useful for other polymers too. The layer by layer deposition of polymer films

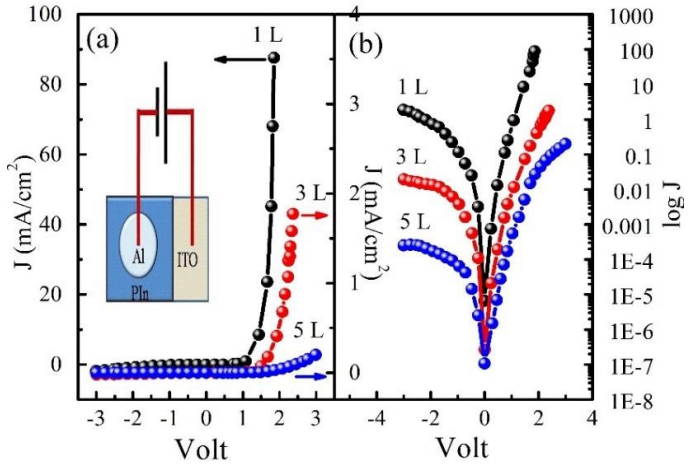

Figure 3.9 (a) J-V characteristics of LB film of PIn single layer (1 L), 3 layers (3 L), and 5 layers (5 L) respectively (b) semilog plot of single layer, 3 layers and 5 layers.

cause the incorporation of an additional conduction mechanism between the layers that not only increases the barrier height along with reduction in reverse saturation current and leakage current, but at the same time also increases the diode turn on voltage with decrease in ideality factor.

3.3 Conclusion

We have successfully fabricated PIn films over various substrates via LB technique exploring its self-organizing property in order to obtain its ordered, uniform and compact film. We obtained stable thin films of unsubstituted PIn over large area without incorporating any insulating surfactant/template that could camouflage its conductivity. We reasonably justified the isotherm obtained for PIn via AFM and SEM characterization and validated 30 mN/m SP as the optimum point for deposition of uniform LB films. Absorption spectra of LB film discloses characteristics absorptions of PIn with 2.9 eV band gap whereas Raman spectra reveals the enhanced ordering in LB film. Furthermore, layer dependent (1, 3 and 5 layers) study of charge transport discloses the deviation in electrical parameter such as ideality factor, barrier height and maximum rectification ratio

for 5 layers due to reduction in leakage current. Thus, our study presents interaction property of unsubstituted PIn over water surface, attainment of stable and large area thin films and layer dependent charge transport with improvement in device performance. The authors feel this work as motivation for LB film preparation of other conductive polymers devoid of alkyl chain that were getting out of research attention.